Conference Paper, Published Version

Bruwier, Martin; Erpicum, Sébastien; Archambeau, Pierre; Pirotton, Michel; Dewals, Benjamin

Mathematical Formulation of Shallow Water Models with Porosity for Urban Flood Modelling

Zur Verfügung gestellt in Kooperation mit/Provided in Cooperation with:
Kuratorium für Forschung im Küsteningenieurwesen (KFKI)

Mathematical Formulation of Shallow Water Models with Porosity for Urban Flood Modelling

M. Bruwier, S. Erpicum, P. Archambeau, M. Pirotton & B. Dewals
Hydraulics in Environmental and Civil Engineering (HECE), University of Liege (ULG), Belgium

ABSTRACT: Due to climate change and other environmental changes such as growing urbanization, floods are expected to become more frequent and severe in the future. However, the magnitude of these changes remains highly uncertain. This calls generally for the analysis of a high number of scenarios and, therefore, many runs of the numerical models are necessary. Simultaneously, high-resolution topographic data have become widely available. Consequently, the present need is mainly for high performance computational models which take full benefit of the available detailed data, combining thus accuracy and high efficiency. One way to meet this challenge is the development of subgrid models. Within each computational cell of a subgrid model, the topography is represented by porosity parameters. The existing approaches for the derivation of the shallow water equations (SWE) with porosity differ in the mathematical formulations obtained, in the assumptions, in the applicability range of the models as well as in the definitions of the porosities (depth-dependent/depth-independent, isotropic/anisotropic). In this paper, we review and compare the different formulations, highlight their respective limitations and criticaly analyse the major assumptions.

Keywords: Urban flood modelling, Porosity, Representative Elementary Volume

1 INTRODUCTION

A detailed modelling flood in urban areas usually requires a fine discretization hardly compatible with computational efficiency. To improve this computational efficiency, one option is the use of coarser grids while preserving some representation of obstacles (i.e. buildings, walls,…) inside the cells.

Some techniques simply rely on the standard shallow water equations (SWE). These include the use of an additional flow resistance to represent the influence of the obstacles (Yu and Lane, 2006a, 2006b, Soares-Frazão et al. 2008). Despite their simplicity, a strong drawback of these techniques is the poor use of the available topographic data (Dottori 2013).

The subgrid parameterization methods enable the available topographic details to be preserved even on coarser grids thanks to the use of porosity parameters. These porosities represent the part of space not occupied by topographic obstacles which are therefore free for water. The presence of these obstacles impacts the volume of water stored and the flux echanges which are respectively represented by storage porosity and conveyance porosity. Some methods use isotropic porosity and therefore do not distinguish the storage porosity from the conveyance one (Guinot and Soares-Frazão 2006, Soares-Frazão et al. 2008) while other methods distinguish both porosities thanks to anisotropic porosity (Sanders et al. 2008, Guinot 2012, Chen 2012a). Chen (2012b) reflects separate flows paths within a cell thanks to a multi-layered approach. Some methods enable to consider the variability of the porosity with the altitude of the free surface thanks to relationship between the free surface and topographic parameters (i.e. volume of water stored, conveyance area, roughness depths) with centered grid (Yu and Lane 2006b, McMillan and Brasington 2007) or staggered grid (Stelling 2012, Volp et al. 2013, Vojinovic et al. 2013).

Each of these methods requires a mathematical reformulation of the SWE. Depending on the authors, the modified SWE are derived in various ways with specific assumptions and limitations.

The present paper firstly reviews the different mathematical formulations used with subgrid methods to model urban floods and highlights the major assumptions and limitations. Then, some major assumptions are critically analysed based on a theoretical example and on a real-word case study.

2 FORMULATIONS OF THE SHALLOW WATER EQUATIONS WITH POROSITY

2.1 *Definition*

To derive the SWE with porosity, the three-dimensional Reynolds equations are space-averaged over a control volume (CV). A control volume can be considered at every local point of the urban area, no matter whether that point corresponds to voids or to an obstacle.

An areal porosity is the fraction of a horizontal plane of a CV free for water at a given altitude. A linear porosity is the fraction of a horizontal line of a border free of water exchanges between the two CV at each sides of the border at a given altitude. The mean linear porosity for a CV is the average of all linear porosities corresponding to smaller CV. It tends toward the areal porosity when the size of the CV increases. The mean linear porosity is the mathematical expectation that a point is free for water, for a given size of the CV.

Chen (2012a,2012b) uses the terms BCR and the CRF to carry out, respectively, the role of the storage and conveyance porosities. The BCR and CRF represent the fraction of space occupied by obstacles and are the complementaries of, respectively, the areal and linear porosities.

The representative elementary volume (REV) is defined as the smallest size of a CV for which the porosities are independent of the size of this CV. Differential SWE equations with porosity are derived with the assumption that the size of the CV exceeds the size of the REV. This assumption turns the porosities into parameters independent of the size of the CV.

2.2 *Shallow water equations with porosity for partially dry areas*

SWE with porosity were presented by Defina (2000) to deal with partially wet and very irregular domains. The derivation is performed by volume-averaging the three-dimensional Reynolds equations over the horizontal projection of a REV and then over the water depth. Consequently to the averaging process, the inertial term of the differential form of the continuity equation is multiplied by a depth-dependent storage areal porosity. Moreover, an additional term appears in the momentum equation due to velocity fluctuations induced by the bottom unevenness. Defina highlights the major assumptions and difficulties related to the use of SWE with porosity in a subgrid model; i.e. the assumption of the existance of a REV smaller than the size of the CV, the assumption of a smoothly varying free surface level inside the mesh, the assumption of full connectivity within each cell and the difficulties to evaluate both the stresses induced by the velocity fluctuation insides the cell and the stresses at the bottom when the flow concentrates along specific paths.

2.3 *Differential Formulation*

Guinot and Soares-Frazão (2006) derived a differential formulation of the SWE with depth-independent isotropic porosity, which was later applied for urban flood modelling (Soares-Frazão et al. 2008). In this derivation, the space-averaging is first performed along the water depth and then over the area of the horizontal projection of the CV. Then, the differential formulation is obtained from the integral one by letting the size of the CV tends towards zero. The isotropic porosity is assumed to be a statistical property representing both the storage volume and the conveyance sections due to the presence of obstacles. To derive the differential formulation from the integral one, the porosity is assumed continuous and differentiable.

Lhomme (2006) extended the differential formulation of Guinot and Soares-Frazão (2006) to depth-independent anisotropic porosities. Besides the storage areal porosity, conveyance linear porosities are introduced and assigned to the border fluxes. However, these anisotropic porosities were not properly defined by Lhomme (2006) and the resulting equations were derived theoretically; but not applied to urban flood modelling.

The three assumptions of continuous, differentiable and isotropic porosity required to derive the differential formulation of the SWE with porosity are all verified if the size of the CV for which porosities are computed is higher than the size of the REV (Sanders 2008). In this approach, the porosities are consid-

ered as mathematical expectation values of the presence of void at the scale of the REV. Based on theoretical Cartesian and periodic streets networks, Guinot (2012) shows that the REV does not exist for real-word urban areas. However, he argues that the error on the isotropic porosity evaluation is of the same order of accuracy as other errors in the model, such as the friction coefficient. According to Guinot (2012), this enables the use of the differential formulation to model urban floods with a reasonable accuracy.

Guinot (2012) described a multiple porosity model in which the domain is subdivised into five types of region. These regions correspond, respectively, to obstacles without voids, regions with water at rest, regions of isotropic 2D flow, regions of anisotropic 1D flow and interconnections between the 1D anisotropic flow regions. These regions may exchange mass and momentum based on local differences in, repectively, water levels and energy heads. The differential governing equations are directly derived from the formulation derived by Guinot and Soares-Frazão (2006), but, in each type of region, the computation of water depth, flow velocity and depth-independent porosity are distinguished. The multiple porosity models give more accurate results than the classical porosity model but the determination of the different regions is complex for real-world urban areas.

Velickovic (2012) proposed a new formulation of the SWE with depth-independent isotropic porosity, in which the anisotropy of the urban area is taken into account through a closure expression including drag and dispersion terms in the momentum equation. However, Velickovic (2012) acknowledges that these closure relations turn out to be inappropriate to reproduce real-worl anisotropic phenomena.

A multi-layered model was developed by Chen et al. (2012b) to reflect separated flow paths within a single coarse cell. The equations used are 2D non-inertia SWE with BCR and CRF to reflect the cell's porosities (Chen 2012a). Among others, Cea et al. (2010) showed that fully dynamic two-dimensional models give better results than simplified descriptions such as diffusive wave-based description for urban flood modelling.

2.4 *Integral formulation*

The direct discretization of the integral formulation of the SWE with porosity avoids questionable assumptions concerning the size of the REV. After deriving macroscopically the integral formulation of the equations, Sanders et al. (2008) discretized this integral form based on a cell-centered grid and a Godunov-type finite volume method (see also Schubert and Sanders 2012 and Kim et al. 2013). The depth-independent porosities are evaluated for each cell and are therefore direction- and mesh-dependent. Sanders et al. (2008) proved that using anisotropic porosity gives more accurate results than the standard isotropic models. In this model, the fluid pressures acting on the obstacles and on the bottom are lumped into a "quasi-conservative" divergence term, consistently with the method proposed by Valiani and Begnudelli (2006).

Stelling (2012), Volp et al. (2013) and Vojinovic et al. (2013) use finite volume approaches for solving the SWE with porosity based on a staggered grid. The main unknowns are the volume of water stored in a cell and the mean velocity at a border. They associate relationships to the cells and the borders to represent, respectively, the depth-dependency of the storage volumes and the conveyance areas. These relationships are similar to depth-dependent anisotropic porosities and are therefore of relevance for the following of this paper. One benefit of this method is that it does not require to distinguish the obstacles from the ground in a pre-processing step to evaluate the depth-independent porosity.

3 CRITICAL ANALYSIS OF SOME MAJOR ASSUMPTIONS OF THE EXISTING FORMULATIONS

The majority of the standard formulations of the SWE with porosity are derived under the assumption of a depth-independent porosity. Moreover, the two additional assumptions of continuity and differentiability of the flow variables are used for the differential formulations, as well as the assumption that the size of the CV is higher than the size of the REV. Then, the absence of a proper definition of an anisotropic porosity in the differential formulations leads to the use of an isotropic porosity by many authors. These major assumptions are analysed in this section based on theoretical and real-world urban areas.

3.1 Method

Guinot (2012) analysed the sizes of REV for theoretical periodic Cartesian urban networks with depth-independent porosities. The widths W of the streets and of the obstacles $W_b=L-W$ were considered as variable parameters to account for multiple city geometries (Figure 1-a). The extent of the urban area was assumed infinite in all directions. Such analyses have been extended and generalized in the scope of the present research, considering not only theoretical urban network; but also a real-word case study (center of Liege, Belgium), involving depth-dependent porosities (Figure 1-b).
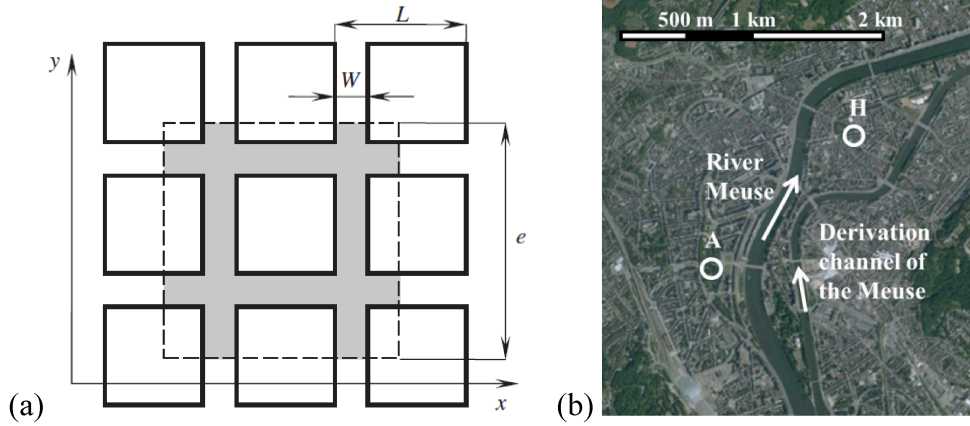

Figure 1. (a) Excerpt of the periodic Cartesian urban network defined by Guinot (2012). (b) Aerial picture of the city of Liege, Belgium, with the localization of Boulevard d'Avroy (A) and Rue Henri Dinant (symbol H).

We define the size of the REV as the size of the CV for which the relative porosity error Φ_{err} is lower than a threshold percentage $X\%$:

$$\phi_{err} = \frac{\phi - \phi_{REV}}{\phi_{REV}} < X\%$$

(1)

with ϕ_{REV} the asymptotic porosity and ϕ the porosity for a given size of the CV.

3.2 Results and discussions

3.2.1 Representative elementary volume

For each possible configuration of the theoretical streets networks ($W/L \in [0,1]$) and each position of the CV, the computed areal porosity oscillates around an asymptotic areal porosity value, which is reached asymptotically, as depicted in Figure 2 for a point situated in the center of gravity of an obstacle block. The evolution of the non-dimensional size of the REV $(e/L)_{X\%}$ as a function of the ratio between the street length over the obstacle length W/L is presented in Figure 3 for different threshold percentages $X\%$.
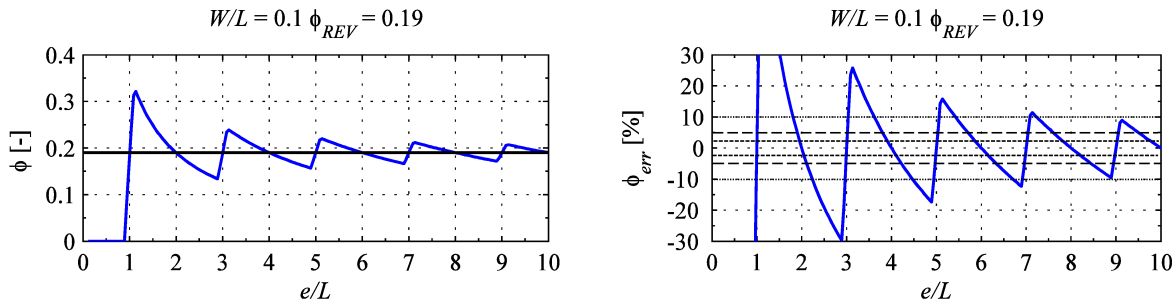

Figure 2. Evolution of the areal porosity and the relative porosity error for a point situated in the center of gravity of an obstacle block.
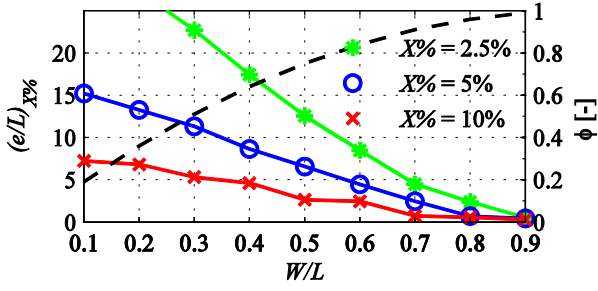
Figure 3. Evolution of the size of the REV and of the areal porosity (dashed line) as a function of the streets network configuration.

Figure 3 indicates that the smaller the porosity, the larger the size of the REV. For the lower values of W/L, the size of the REV is high because a small variation of the porosity induces an important relative variation due to the low porosity value. In this research, we focus on floods in urban areas, for which the values of W/L are generally low. Therefore, the size of the REV is high. For example, with a spatial length L of 200 m and a threshold percentage of 5%, the edge dimension of a squared control volume has to be higher than 1.3 km to verify the assumption of a continuous media for a W/L value of 0.5 ($\phi_{REV} = 0.75$).

For the urban area of Liege, the areal porosities do not converge towards finite values due to the irregular urban patterns. The evolutions of the depth-dependent areal porosity with the size of the CV are represented in Figure 4 for Boulevard d'Avroy (A), localized in Figure 2-b. To show the influence of the depth-dependency, six areal porosities are determined for six altitudes between the ground surface levels to altitudes above the maximum range of water levels.
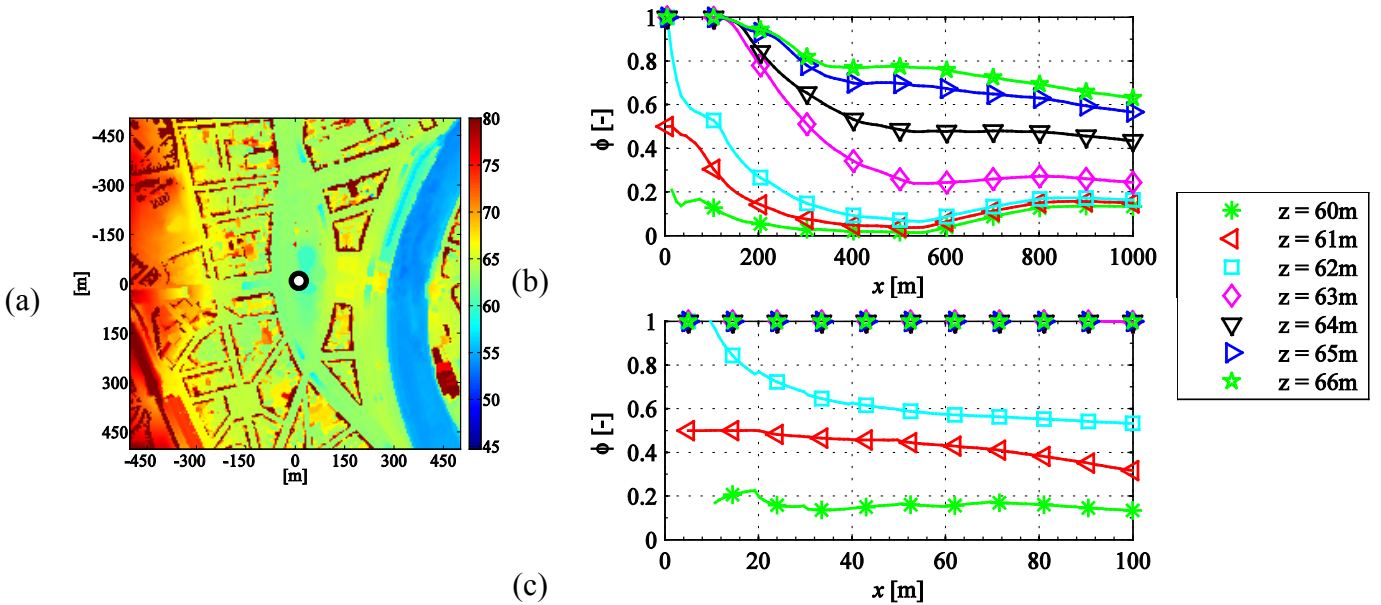

Figure 4. Evolution of the depth-dependent areal porosities for increasing size of the CV, centered on Boulevard d'Avroy (A).

The irregular patterns of the urban networks do not guaranty a convergence of the porosity when the size of the control volume increases for Boulevard d'Avroy (A). A REV cannot be defined below practical CV sizes (10-100 m) and the use of a single depth-independent porosity, like in most existing approaches, is here strongly arguable.

3.2.2 Continuity and differentiability of the porosities

For the theoretical streets network, the areal porosities were computed at each point situated between points A ($x = 0$) and B ($x = 1$), for different CV sizes (Figure 5-a). The street network is characterized by the same street and obstacle widths ($W/L = 0.5$). As demonstrated in Figure 5-b, the porosity shows substantial variations at $x = 0.25$ and $x = 0.75$ for the smallest CV, which is much smaller than the REV. When the size of the CV increases, the spatial variation of the areal porosity decreases because this porosity converges towards the asymptotic value ϕ_{REV}.
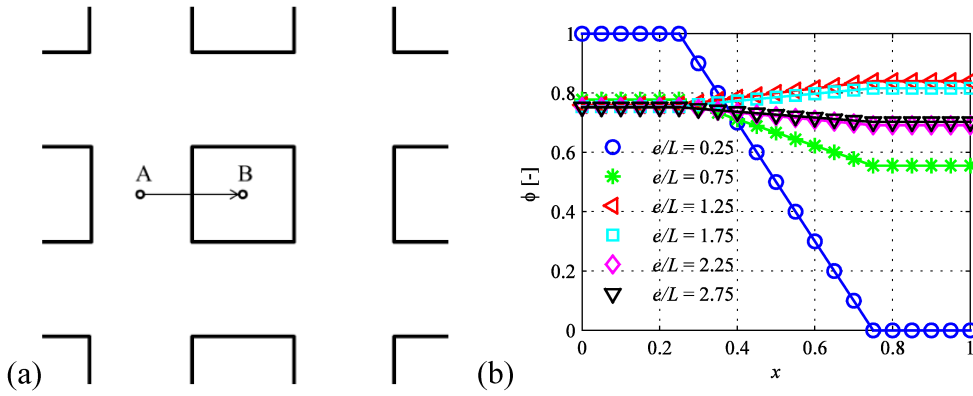
Figure 5. (a) Areal porosities are computed for points situated between A ($x = 0$) and B ($x = 1$). (b) The spatial variation of the areal porosity between points A and B is presented for different CV sizes.

For the city of Liege, the spatial variation of the areal porosity near Rue Henri Dinant (H) is shown in Figure 6. From a digital surface model (DSM) with a mesh-resolution of 5 m, the areal porosity is calculated for each topographic cell along X and Y directions on either sides of the considered point. The CV size varies between the size of the topographic cell to 50 m. The areal porosity is depicted in the following figures at an altitude corresponding to an average water depth around 1 m, i.e. $z = 63$ m. Continuous lines show areal porosities calculated for each topographic cell (the CV is translated by 5 m). The dotted line is the porosity variation from one computational cell to its neighbor, i.e. the CV is translated by its size (50 m).

When the size of the CV is the size of the topographic cell, the porosity is binary: either the cell is free for water or not. The porosity is highly discontinuous. When the size of the CV increases, the variations of porosity become more continuous. Nonetheless, the variation of porosity from one computational cell to its neighbors (dashed bold line) is abrupt and represents relatively poorly the porosity variation inside the computational cells (plain line).
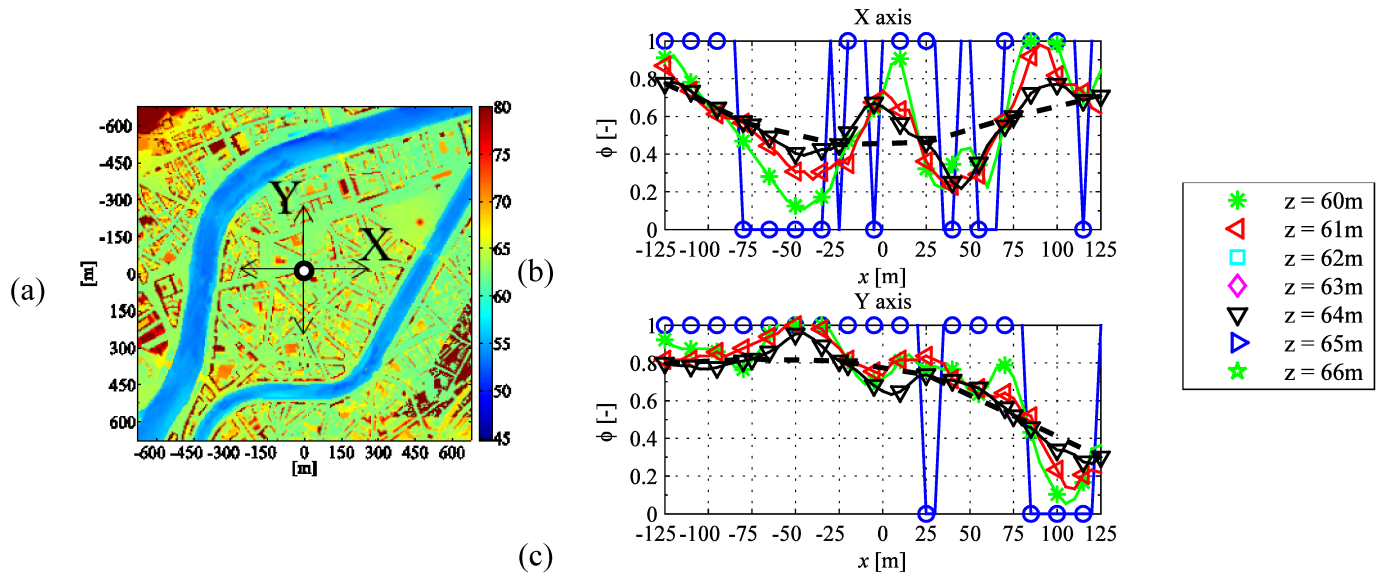

Figure 6. Spatial variation of the areal porosity at $z = 63$ m around Rue Henri Dinant (H).

3.2.3 *Isotropic and anisotropic porosities*

Consider the theoretical street network with two configurations of the street and obstacle widths ($W/L = 0.1$ and $W/L = 0.5$). The linear and areal porosities are computed for different CV sizes and for a point situated at the center of gravity of an obstacle block.

In Figure 7, the linear porosity (plain line) is highly discontinuous and fluctuates around the areal porosity without converging. The mean linear porosity converges slowly toward the areal porosity when the size of the CV increases. Despite this, for equal street and obstacle widths, the mean linear porosity is slighly (maximum 7%) higher than the areal porosity when the size of the CV reaches the size of the REV (threshold percentage of 5%). For the ratio $W/L = 0.1$, the maximum difference reaches around 30% for the same threshold percentage. So, even at the scale of the REV, replacing the mean linear porosities by the areal porosity remains questionable.
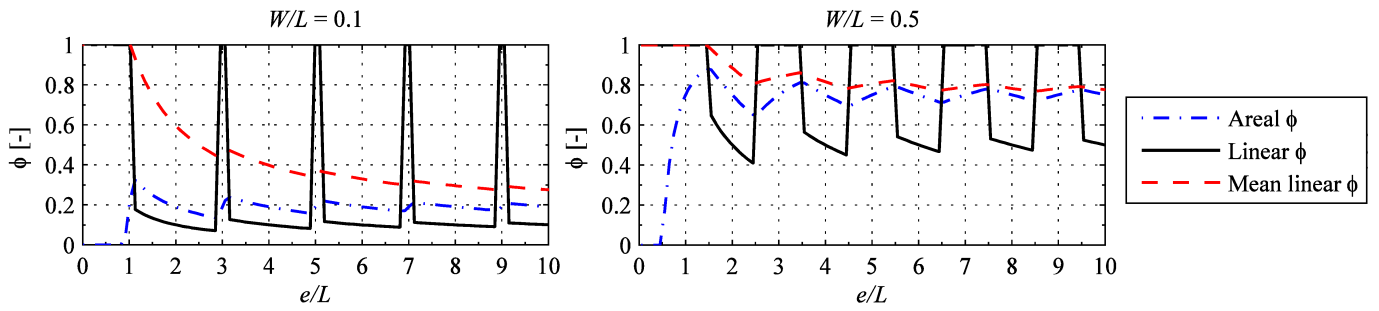
Figure 7. Evolution of areal, linear and mean linear porosities as a function of the size of the CV for a point situated in the center of gravity of an obstacle block.

For Rue Henri Dinant (H) in the city of Liege, the linear porosity is computed at a border of the CV as the areal porosity of the area centered on the mid-point of the border with a length equal to the border length and the other equal to the topographic cells (5 m) (Figure 8-a).
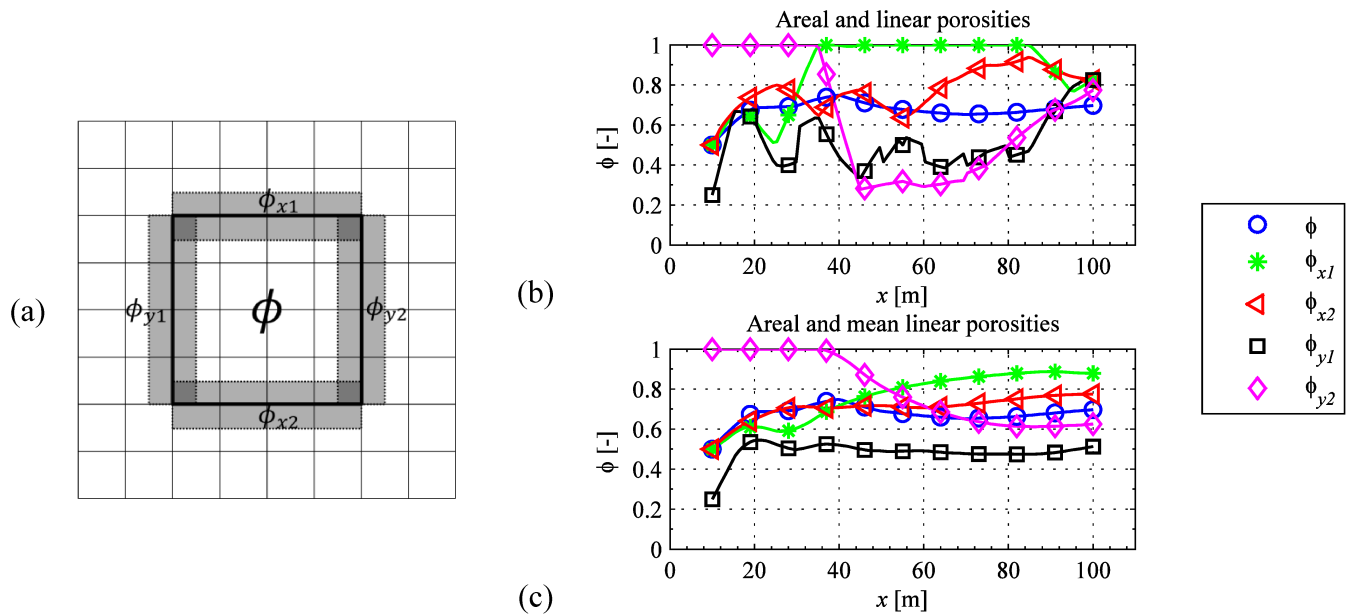

Figure 8. (a) Computation of the linear porosity at the borders of the CV. (b-c) Evolution of areal, linear and mean linear porosities as a function of the size of the CV for a point situated in the center of gravity of an obstacle block.

In Figure 8-b, the areal porosity of a CV is compared to the linear porosities at each four borders of the CV. In this figure, the linear porosities are, logically, far more sensitive to the size of the CV than the areal porosity. The anisotropic linear porosities are highly different from one border to the other and from the areal porosity.

For the mean linear porosities (Figure 8-c), the sensitivity to the size of the CV is logically lower when the size of this CV increases. However, the mean linear porosities remain different from one border to the other and compared to the areal porosity, thereby showing the anisotropy of the urban area.

4 CONCLUSION

The article reviews the litterature concerning urban flood modelling with the SWE involving porosities. The different derivations of the SWE with porosity are critically analysed in terms of required assumptions and limitations of application. To derive the differential formulation of the SWE with porosity, the porosity is usually assumed continuous, differentiable and, in most cases, isotropic. This implies the existence of a representative elementary volume (REV) smaller than the computational cell. Based on quantitative analyses for theoretical and real-word urban areas, it has been shown that none of these assumptions can be fulfilled for usual cell sizes as used in practice. Moreover, the results call for the use of anisotropic porosity and for the evaluation of the porosity as a discrete cell-property rather than a continuous mathematical field. Finally, the use of depth-independent porosity does not allow the consideration the submersion of obstacles and requires a pre-treatment to distinguish the obstacles from the ground in the digital surface model.

165

REFERENCES

Cea, L., M. Garrido and J. Puertas (2010). Experimental validation of two-dimensional depth-averaged models for forecasting rainfall-runoff from precipitation data in urban areas. Journal of Hydrology 382(1-4): 88-102.

Chen, A. S., B. Evans, S. Djordjević and D. A. Savić (2012a). A coarse-grid approach to representing building blockage effects in 2D urban flood modelling. Journal of Hydrology 426–427(0): 1-16.

Chen, A. S., B. Evans, S. Djordjević and D. A. Savić (2012b). Multi-layered coarse grid modelling in 2D urban flood simulations. Journal of Hydrology 470–471(0): 1-11.

Defina, A. (2000). Two-dimensional shallow flow equations for partially dry areas. Water Resources Research 36(11): 3251-3264.

Dottori, F., G. Di Baldassarre and E. Todini (2013). Detailed data is welcome, but with a pinch of salt: Accuracy, precision, and uncertainty in flood inundation modelling. Water Resources Research 49(9): 6079-6085.

Guinot, V. and S. Soares-Frazão (2006). Flux and source term discretization in two-dimensional shallow water models with porosity on unstructured grids. International Journal for Numerical Methods in Fluids 50(3): 309-345.

Guinot, V. (2012). Multiple porosity shallow water models for macroscopic modelling of urban floods. Advances in Water Resources 37: 40-72.

Kim, B., B. F. Sanders, J. E. Schubert and J. S. Famiglietti (2014). Mesh type tradeoffs in 2D hydrodynamic modelling of flooding with a Godunov-based flow solver. Advances in Water Resources 68: 42-61.

Lhomme, J. (2006). Modélisation des inondations en milieu urbain: approches unidimensionnelle, bidimensionnelle et macroscopique. PhD Thesis, Université de Montpellier II.

McMillan, H. K. and J. Brasington (2007). Reduced complexity strategies for modelling urban floodplain inundation. Geomorphology 90(3-4): 226-243.

Sanders, B. F., J. E. Schubert and H. A. Gallegos (2008). Integral formulation of shallow-water equations with anisotropic porosity for urban flood modelling. Journal of Hydrology 362(1-2): 19-38.

Schubert, J. E. and B. F. Sanders (2012). Building treatments for urban flood inundation models and implications for predictive skill and modelling efficiency. Advances in Water Resources 41(0): 49-64.

Soares-Frazão, S., J. Lhomme, V. Guinot and Y. Zech (2008). Two-dimensional shallow-water model with porosity for urban flood modelling. Journal of Hydraulic Research 46(1): 45-64.

Stelling, G. S. (2012). Quadtree flood simulations with sub-grid digital elevation models. Proceedings of the Institution of Civil Engineers: Water Management 165(10): 567-580.

Velickovic, M. (2012). Macroscopic modelling of urban flood by a porosity approach. PhD Thesis, Université catholique de Louvain (UCL).

Vojinovic, Z., S. Seyoum, M. H. Salum, R. K. Price, A. K. Fikri and Y. Abebe (2013). Modelling floods in urban areas and representation of buildings with a method based on adjusted conveyance and storage characteristics. Journal of Hydroinformatics 15(4): 1150-1168.

Volp, N. D., B. C. Van Prooijen and G. S. Stelling (2013). A finite volume approach for shallow water flow accounting for high-resolution bathymetry and roughness data. Water Resources Research 49(7): 4126-4135.

Yu, D. and S. N. Lane (2006a). Urban fluvial flood modelling using a two-dimensional diffusion-wave treatment, part 1: Mesh resolution effects. Hydrological Processes 20(7): 1541-1565.

Yu, D. and S. N. Lane (2006b). Urban fluvial flood modelling using a two-dimensional diffusion-wave treatment, part 2: Development of a sub-grid-scale treatment. Hydrological Processes 20(7): 1567-1583.